HUE
HORUS UNIVERSITY - EGYPT
HORUS UNIVERSITY JOURNAL OF ENGINEERING
JOURNAL HOMEPAGE: HTTPS://HUJE.JOURNALS.EKB.EG/
ONLINE ISSN: 3062-4991
HUJE

Article

Numerical and Regression-Based Modeling of Leakage in Lined Trapezoidal Channels

Mohamed Kamel Elshaarawy[1,*]

[1]Civil Engineering Department, Faculty of Engineering, Horus University-Egypt, New Damietta 34517, Egypt; melshaarawy@horus.edu.eg; ORCID: https://orcid.org/0000-0002-1793-5617

[*] Corresponding author

ABSTRACT

Leakage losses in unlined and lined trapezoidal channels are critical factors influencing water conservation and infrastructure efficiency. This study employs the Slide2 numerical model to estimate leakage losses and develop multiple-nonlinear-regression (MNR) models for predictive analysis. A validation process was conducted by comparing the analytical solution with the Slide2 model, showing excellent agreement with a minimal deviation of 3%–6% across different canal geometries. The simulation results highlight the significant effects of channel bed width-to-water depth ratio ($b^*=b/y$), liner-to-soil hydraulic conductivity ratio ($k^*=k_L/k$), liner thickness-to-water depth ratio ($t^*=t_L/y$), and side slope (z) on leakage losses. It was observed that increasing t_L led to a reduction in leakage by as much as 68%, while lowering k_L substantially decreased losses, with almost complete elimination occurring when k^* was less than or equal to 0.01. A set of MNR equations was developed for different side slopes, achieving R^2 values exceeding 0.89, confirming high predictive performance. A generalized equation applicable to all side slopes was also formulated, achieving a determination coefficient (R^2) of 0.899 with a root-mean-squared-error (RMSE) of 1.448. The accuracy of the model was additionally confirmed through scatter plots, which showed that the predicted values closely aligned with the actual leakage losses. Finally, the findings confirmed the reliability of the Slide2 model for leakage loss estimation and underscore the importance of liner properties in water conservation. The developed regression models provided a practical tool for predicting leakage losses, aiding in the design and optimization of lined canals.

ARTICLE HISTORY

Received: 08 March 2025
Revised: 28 April 2025
Accepted: 15 May 2025

KEYWORDS

Finite element model
Groundwater Modeling
Leakage
Lining
Nonlinear Regression
Slide2 model
Trapezoidal channel

HIGHLIGHTS

- Slide2 model accurately predicts leakage losses in trapezoidal channels with minimal error.
- MNR equations developed for varying side slopes achieve R^2 values above 0.89.
- Liner properties significantly impact leakage losses; lower k^* and higher t^* reduce seepage.
- Side slope variation has a minor effect on leakage losses compared to liner properties.
- Generalized MNR model with R^2 of 0.899 and RMSE of 1.448 predicts leakage across all side slopes.

GRAPHICAL ABSTRACT

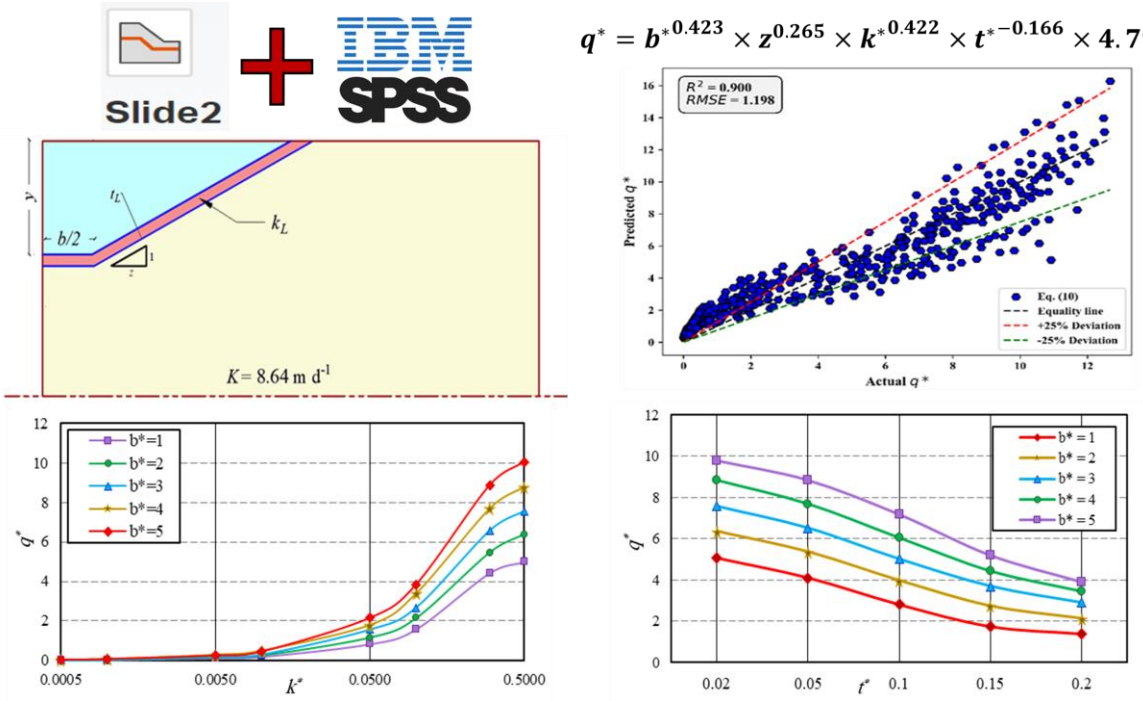

ABBREVIATIONS

ANN	Artificial Neural Network
ANOVA	Analysis of Variance
CC	Cement Concrete
FEM	Finite Element Method
LDPE	Low-Density Polyethylene
MLPNN	Multilayer Perceptron Neural Network
MNR	Multiple Nonlinear Regression
RBFNN	Radial Basis Function Neural Network
RR	Random Rubble
VIF	Variance Inflation Factor

1. Introduction

LEAKAGE is the main source of water loss in irrigation channels, occurring when water moves through the bed and sides of the channel [1]. This water infiltrates vertically and spreads laterally into the surrounding soil, leading to a reduction in the available water for irrigation [2]. As a result, the efficiency of water conveyance systems decreases [3]. Such leakage losses can disrupt the timely and equitable distribution of water, which is essential for fulfilling agricultural needs [4].

Moreover, leakage may raise unconfined groundwater levels, causing water to rise through, waterlogging, capillary action, resulting in soil saturation and salt accumulation in the root zone, which negatively affects crop yields [5]. In areas with fallow land or natural vegetation, high groundwater levels can contribute to non-beneficial water consumption through evaporation and transpiration by weeds and phreatophytes [6]. Additionally, leakage impacts the subsurface return flow into channels, further diminishing the efficiency of water conveyance systems and highlighting the importance of effective leakage management in water resource planning [7].

Various techniques are utilized to mitigate leakage in irrigation channels, including channel lining, soil compaction, and sealing [8]. Although empirical equations and analytical models based on parameters such as channel discharge, flow velocity, and soil hydraulic properties are commonly employed, numerical modeling has gained prominence due to its efficiency and reduced dependence on extensive datasets [9]. Among these techniques, channel lining has been identified as particularly effective in minimizing water loss. Different types of liners, including compacted soil, soil-cement mixtures, asphaltic concrete, flexible membranes, and conventional concrete, serve as effective barriers against seepage [10]. In addition to reducing leakage, channel lining enhances hydraulic efficiency, lowers maintenance costs, suppresses weed proliferation, and prevents waterlogging in nearby agricultural areas [11], [12].

Extensive research has been conducted to evaluate the performance of various liners in reducing seepage losses, providing critical insights into their long-term efficiency and limitations [13], [14]. Advances in modeling techniques have significantly enhanced the ability to analyze leakage in irrigation channels. For example, hybrid modeling approaches have demonstrated superior accuracy in predicting seepage in irrigation systems [15]. Beyond computational modeling, both geometric and hydraulic characteristics significantly impact leakage rates. For instance, increased hydraulic conductivity, greater freeboard, steeper slopes, and higher channel walls have been observed to elevate leakage in triangular channels, highlighting the necessity of considering both liner selection and channel design [16]. Further investigations into trapezoidal, rectangular, and triangular channels using SEEP/W

software have identified the wetted perimeter as a critical factor affecting seepage rates, whereas the influence of side slopes has been found to be relatively minor [17]. These findings underscore the importance of integrating material properties and structural design considerations in the development of effective leakage management strategies.

Finite element modeling has been widely applied to assess leakage losses in both lined and unlined trapezoidal channels. Hosseinzadeh Asl et al. [16] developed linear and nonlinear multivariate relationships to analyze leakage in trapezoidal, rectangular, and triangular channels. Their results reaffirmed that wetted perimeter was a key determinant of leakage, while side slopes had a lesser impact. Salmasi and Abraham [17] further investigated the role of hydraulic and geometric parameters using SEEP/W and empirical relationships, confirming that SEEP/W provided more precise leakage estimates, whereas empirical methods exhibited significant errors. Solomon and Ekolu [18] demonstrated that the effectiveness of a channel lining in reducing leakage is largely dependent on its permeability. Their findings revealed that leakage reduction was maximized when the ratio of concrete lining permeability to subsoil permeability ranged between 6.9×10^{-5} and 5×10^{-5}. While increasing the lining thickness had a relatively minor effect, it was recommended that thickness should not exceed 75 mm.

Similarly, Jamel [19] investigated leakage in both lined and unlined triangular channels using SEEP/W, concluding that seepage rates increased with higher hydraulic conductivity of both the soil and lining materials. Additionally, leakage was found to rise with an increase in freeboard, side slope steepness, and overall channel height, which is defined as the combined depth of water and freeboard. Tavakoli et al. [20] compared empirical equations with SEEP/W simulations in the Boldaji earth channel in Iran, concluding that the Moritz equation provided the closest and most accurate leakage estimates. However, SEEP/W was particularly effective for modeling trapezoidal cross-sections.

Beyond leakage control, optimizing channel design is crucial for minimizing water losses while maintaining cost efficiency. Since channel construction costs include both direct expenses (such as excavation and lining materials) and indirect costs (such as leakage and evaporation losses), optimization techniques have been developed to determine the most cost-effective channel dimensions while ensuring hydraulic stability. MATLAB-based optimization algorithms have been applied to achieve this balance, incorporating constraints such as minimum permissible velocity and Froude's number to maintain stable flow conditions [21]. These studies emphasize the importance of integrating leakage reduction strategies into cost-effective channel design. Furthermore, accurate leakage estimation plays a key role in optimization, as traditional empirical equations often introduce errors. To address this limitation, another study used SEEP/W modeling to simulate leakage under various channel configurations and developed a soft computing model that correlates channel geometry and soil properties with leakage losses [22]. This approach proved to be more reliable than conventional empirical equations, offering a more effective framework for estimating leakage in cost-optimization studies.

Channel liners play a vital role in mitigating leakage losses in irrigation systems. Comparative studies examining channels lined with random rubble (RR) masonry and low-density polyethylene (LDPE) indicate that LDPE liners are significantly more effective, reducing leakage losses to approximately 2%, in contrast to 8% observed with RR liners [23]. These findings highlight the necessity of selecting appropriate lining materials based on specific leakage reduction objectives and operational requirements. Unlined channels also serve as critical benchmarks for evaluating the efficiency of lined systems. Notably, the SEEP/W model has demonstrated superior accuracy in predicting leakage losses compared to conventional empirical methods, which often yield considerable errors [16].

Research on compacted earth linings has demonstrated that highly compacted soils can reduce leakage discharge by as much as 99.8%, emphasizing the importance of thorough channel surface preparation [24]. Furthermore, studies have established that the hydraulic conductivity of the lining material is the most influential factor affecting leakage rates, irrespective of variations in groundwater table depth or channel berm width. This underscores the need to select liners with optimal hydraulic properties to ensure effective and long-term leakage prevention [5]. Additionally, an analysis of the El-Sont Channel in Egypt, utilizing Slide2 and FLOW-3D models, revealed that cement concrete (CC) and LDPE linings can achieve leakage reductions of up to 97%, while simultaneously increasing channel discharge by an average of 150% [25].

In recent years, predictive modeling techniques have become indispensable for simulating hydraulic and hydrological processes [25]–[29]. These models are particularly advantageous in handling complex and noisy datasets, making them highly suitable for leakage analysis, which can be challenging to model using conventional physical methods. For instance, comparative studies on leakage losses in unlined and lined channels have demonstrated that Gene Expression Programming (GEP) surpasses Artificial Neural Networks (ANN) in predictive accuracy, further reinforcing the value of advanced computational approaches in irrigation channel analysis [30]. Multilayer Perceptron Neural Network (MLPNN) has been identified as the most reliable model for predicting leakage loss, consistently performing well across different training-to-testing data splits [25]. Additionally, the Radial Basis Function Neural Network (RBFNN) has been recognized as the most accurate model for estimating leakage loss in lined trapezoidal channels [31].

Despite previous studies addressing the influence of side slopes, liner hydraulic conductivity, and thickness on leakage from lined trapezoidal channels, most have relied on field

observations or experimental models without developing generalized predictive tools. Moreover, no study has formulated MNR equations that explicitly account for varying side slopes to estimate leakage losses directly and accurately. Existing approaches often involve indirect methods and approximations, which may introduce significant errors. Therefore, the main objective of this study is to develop and validate accurate MNR models based on numerical simulations, enabling the direct prediction of leakage losses from lined trapezoidal channels under different geometric and hydraulic conditions. These models are intended to serve as a practical and reliable tool for hydraulic engineers and water resource managers to optimize canal design and enhance water conservation.

2. Materials and Methods

2.1. Groundwater Leakage Modeling

Slide2 software is a widely used limit equilibrium-based slope stability analysis developed by Rocscience [32]. It enables 2D numerical modeling of groundwater leakage within soil and rock slopes by incorporating leakage forces and pore water pressures into stability calculations [33]. The software integrates finite element groundwater flow modeling, allowing for a comprehensive assessment of groundwater movement and its impact on slope stability. The groundwater leakage module in Slide2 allows users to model various hydraulic boundary conditions, including infiltration, perched water tables, and transient leakage. Slide2 solves both steady-state and transient (unsteady-state) leakage problems using the finite element method (FEM).

2.1.1. Governing equation

The governing equation for groundwater leakage in Slide2 is derived from the conservation of mass (continuity equation) combined with Darcy's Law. Darcy's Law describes the movement of water through a porous medium and is fundamental to leakage analysis [5]. Eq. (1) states that the specific discharge (q), also known as the leakage velocity, is proportional to the hydraulic gradient and is given as follows.

$$q = -K\Delta h \tag{1}$$

where q is the specific discharge (m/s), K is the hydraulic conductivity (m/s), h is the hydraulic head (m), and Δh represents the hydraulic gradient, which is the change in head per unit distance. Darcy's Law states that groundwater flow occurs in response to a hydraulic gradient, and the rate of flow is directly proportional to the permeability of the soil or rock medium. For steady-state groundwater flow conditions, the continuity equation (mass conservation) and Darcy's Law combine to form Laplace's Eq. (2).

$$\frac{\partial}{\partial x}\left(K_x \frac{\partial h}{\partial x}\right) + \frac{\partial}{\partial y}\left(K_y \frac{\partial h}{\partial y}\right) = 0 \tag{2}$$

where K_x and K_y are the hydraulic conductivities in the x- and y-directions (m/s), and h is the total hydraulic head (m). This equation governs the distribution of pore water pressures and hydraulic gradients within the soil or rock under steady-state flow conditions, where the groundwater flow remains constant over time. In this study, the Slide2 model is utilized to estimate the leakage discharge in lined channels per unit channel length in a 2D slope system [34].

2.1.2. Effective parameters

The study incorporated various parameters, as illustrated in Figure 1. They are leakage loss per unit length of the channel (q) including liner characteristics (liner thickness, t_L, and hydraulic conductivity, k_L), channel geometry (water depth, y, bed width, b, and side slope, z), and the hydraulic conductivity of the surrounding soil (k).

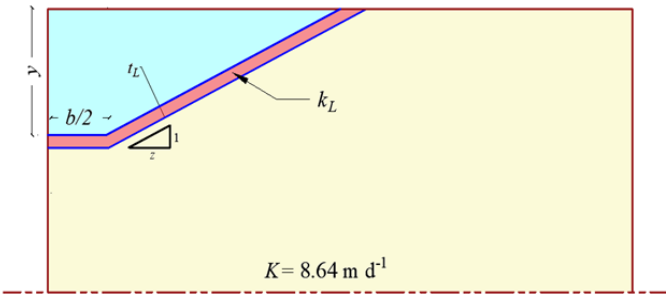

Figure 1. Sketch of a lined trapezoidal channel.

Using dimensional analysis, Eq. (3) is derived to represent the functional relationship between the key parameters influencing leakage loss from lined trapezoidal channels:

$$\phi(b, y, z, k, k_L, t_L, g, q) = 0 \tag{3}$$

The studied problem involves eight variables (n=8). While there are three fundamental dimensions (m=3), ρ, y, and k are selected as the repeated variables by applying Buckingham's π-theorem [35]. Thus, the total number of dimensionless parameters (π-terms) is determined to be five, as shown in Eq. (4).

$$\begin{aligned} &\phi(\pi_1, \pi_2, \pi_3, \pi_4, \pi_5) = 0 \\ &\rightarrow \phi\left(\frac{b}{y}, z, , \frac{k_L}{k}, \frac{t_L}{y}, \frac{q}{ky}, \frac{gy}{k^2}\right) = 0 \end{aligned} \tag{4}$$

As indicated in previous similar studies [4], [24], [31], [36]–[38], the parameters g, k, and y are considered constant. Consequently, the dimensionless term gy/k^2 remains independent of the other variables and is excluded from further analysis, leading to the final form of the equation as presented in Eq. (5).

$$\begin{aligned} &\frac{q}{ky} = \phi\left(\frac{b}{y}, z, \frac{k_L}{k}, \frac{t_L}{y}\right) \\ &\rightarrow q^* = \phi(b^*, z, k^*, t^*) \end{aligned} \tag{5}$$

In Eq. (5), the dependent variable is the leakage loss ratio (q^*), while the independent variables (b^*, z, k^*, t^*).

2.1.3. Model setup

Following the approach outlined by Vedernikov [39], leakage flow was assumed to occur exclusively in the vertical downward direction, with no interaction between leakage and groundwater during the simulation process. To ensure precision

in capturing minor variations in fluxes within the simulation domain, mesh refinement was implemented during the discretization stage. The simulation domain was constructed using three thousand triangular three-noded finite elements, which provided an optimal balance between computational efficiency and accuracy. The setup process began by defining the material properties and dimensions of the unlined channel. Once these parameters were established, the liner's hydraulic conductivity and thickness were specified within the model. The boundary conditions were then incorporated, with the total head boundary condition assigned to the channel perimeter and an exit leakage face condition applied at the bottom of the domain. Following this, a discharge section was designated at a specific location within the model to facilitate the estimation of leakage losses. Upon finalizing the model setup, the leakage analysis was conducted, and the leakage losses at the selected discharge section were extracted for further interpretation. The effective parameters influencing leakage losses, along with the simulation domain and applied boundary conditions, are illustrated in Figure 2.

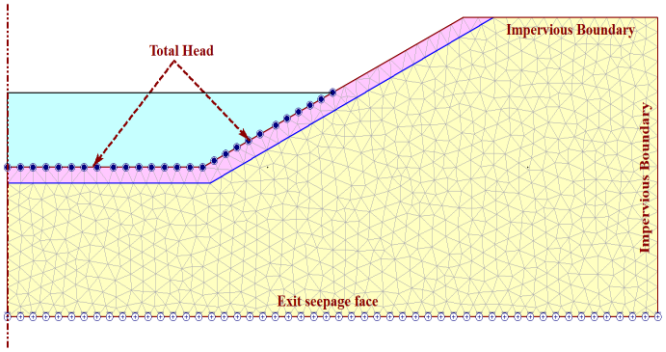

Figure 2. Meshing and boundary conditions utilized in the simulations.

2.1.4. Model validation

The Slide2 model was employed to simulate an unlined trapezoidal channel, commonly referred to as a losing-disconnected channel, flowing through an unconfined, homogeneous, and isotropic porous medium of infinite depth [40]. An analytical approach using the inversion of conformal mapping techniques and hodograph, originally proposed by Vedernikov [39], provides a mathematical solution for leakage losses in such systems. This analytical method considers a trapezoidal channel within an unconfined porous medium and expresses leakage losses using the following Eq. (6):

$$q = k(B + Ay) \quad (6)$$

where q represents leakage losses per unit channel length (m^3 d^{-1} m^{-1}), k is the hydraulic conductivity of the soil (m d^{-1}), B is the top width of the channel (m), and A is a coefficient that depends on the values of B/y and z [41]. In this study, a homogeneous sandy soil with a k of 8.64 m d^{-1} was considered. To validate the Slide2 model, simulations were performed using five different channel geometry ratios (b^* = 1, 2, 3, 4, and 5), where b, y, and z were set as 5m, 5m, and 1H:1V, respectively.

2.1.5. Simulation scenarios

Following the validation process, the influence of both channel geometry and lining on leakage losses is examined to formulate design charts and predictive equations for estimating leakage losses in lined and unlined trapezoidal channels. To achieve this, 600 simulation scenarios for lined channels were conducted using the Slide2 model. These scenarios involved variations in the geometry ratio (b), liner-to-soil hydraulic conductivity ratio (K), and liner thickness-to-water depth ratio (t), with values ranging across b = {1, 2, 3, 4, 5}, z ={1, 1.5, 2}, K = {0.0005, 0.001, 0.005, 0.01, 0.05, 0.10, 0.30, 0.50}, and t = {0.01, 0.05, 0.10, 0.15, 0.20}. These parameter ranges were chosen to reflect real-world channel configurations and commonly encountered values for liner hydraulic conductivity and thickness. To maintain consistency across all simulations, the boundary conditions were defined in accordance with those applied during the calibration phase.

2.2. Multiple Nonlinear Regression Modeling

Multiple Nonlinear Regression (MNR) is a statistical approach used to model complex relationships between dependent and independent variables, particularly when the relationship is non-linear [42]. Unlike linear regression, which assumes a direct proportionality between variables, nonlinear regression accommodates curved, exponential, logarithmic, and polynomial relationships, making it a more suitable technique for capturing intricate patterns in data. In this study, MNR was conducted using IBM SPSS Statistics software [43], which provides a robust framework for estimating parameters in nonlinear models. SPSS employs iterative optimization techniques such as the Levenberg-Marquardt algorithm and quasi-Newton methods to refine parameter estimates and minimize residual errors. The nonlinear model adopted in this study was expressed as previously shown in Eq. (5). The objective was to formulate a regression equation that best represents the relationship between the given variables, ensuring accurate predictions of leakage losses.

To implement MNR in SPSS, the dataset containing normalized independent variables and the dependent variable was first imported, with variables assigned appropriate names for easy identification. The nonlinear regression procedure was then selected through Analyze → Regression → Nonlinear, which opened the regression dialog box where dependent and independent variables were specified. The nonlinear model's functional form was then defined, selecting from power, exponential, logarithmic, or polynomial structures. In this study, a custom nonlinear equation incorporating b^*, z, k^*, and t^* as explanatory variables was implemented.

Once the model structure was established, initial parameter estimates were specified based on previous studies or empirical observations, with values such as b^*=*1*, z=*1*, k^*=0.1, and t^*=0.15. SPSS utilized these initial estimates as a starting point to iteratively adjust and refine the parameters for optimal model performance. Following model definition, the nonlinear

regression process was executed, with SPSS iteratively optimizing the equation using the Levenberg-Marquardt algorithm, minimizing residual errors to achieve the best fit. The output from the MNR analysis included estimated model coefficients, goodness-of-fit statistics such as R^2 and RMSE. A high R^2 value coupled with low RMSE indicated a well-fitting nonlinear model, confirming its effectiveness in capturing the relationship between variables and ensuring reliable leakage predictions [37].

2.3. Multicollinearity and Hypothesis analyses

Regression models rely on the assumption that predictor variables are independent of one another to ensure accurate coefficient estimation and reliable predictions [44]. However, when predictor variables exhibit high correlations, multicollinearity arises, leading to instability in the regression model and inflated standard errors of estimated coefficients. Additionally, assessing the statistical significance of independent variables is crucial to determine their contribution to the predictive model. To address these concerns, this study implemented multicollinearity diagnostics using the Variance Inflation Factor (VIF) and conducted hypothesis testing through Analysis of Variance (ANOVA) and the Z-test.

Multicollinearity was assessed to ensure that predictor variables did not exhibit excessive correlation, which could distort the regression outcomes [45]. To mitigate this issue, min-max normalization was applied, transforming all input variables into a standardized range between 0 and 1, preventing variables with larger scales from disproportionately influencing the regression model [46]. The VIF was then used to quantify multicollinearity, with values below 2.5 indicating weak or negligible correlation and values above 10 suggesting severe multicollinearity, which could compromise model stability

Beyond multicollinearity detection, hypothesis tests were conducted to evaluate the statistical significance of the input variables [47]. ANOVA was used to analyze the contribution of each independent variable to the total variance of the dependent variable. This method decomposed the total variance into explained and unexplained components, with the F-statistic used to assess whether an independent variable had a significant effect on the dependent variable. A high F-statistic and a p-value below 0.05 indicated that the variable meaningfully influenced the regression model [48].

To further validate statistical significance, the Z-test was performed to compare the sample means of input variables against a hypothesized mean, typically set at zero. The Z-score was computed as the ratio of the difference between the sample and hypothesized mean to the standard error of the mean [49]. A p-value below 0.05 confirmed that an input variable significantly deviated from the hypothesized mean, reinforcing its importance in the analysis. Both one-tailed and two-tailed p-values were computed to examine directional and non-directional significance, offering deeper insights into the strength and consistency of the statistical findings [50].

3. Results and Discussion

3.1. Validation process

Table 1 presents a comparative analysis between the calculated values of q^*obtained using Eq. (6) and the Slide2 model across different channel geometry ratios (b^*). The results show a good agreement between the analytical equation and the numerical model, confirming the reliability of the Slide2 model in predicting leakage losses. For all b^* values ranging from 1 to 5, the leakage losses estimated by the Slide2 model are slightly higher than those derived from the analytical equation. This discrepancy may be attributed to the finite element numerical approach in Slide2, which captures complex leakage patterns and hydraulic interactions more comprehensively than the simplified analytical model. The percent difference between the two methods is minimal, with Slide2 values exceeding the analytical estimates by approximately 3% to 6%, indicating good model validation.

Additionally, the leakage loss ratio (q^*) shows an increasing trend with higher b^* values, reflecting the expected behavior where wider channels experience greater leakage due to the expanded wetted perimeter. The relative difference in q^* between Eq. (6) and Slide2 remains consistent, reinforcing the numerical model's robustness in simulating leakage losses accurately. Overall, the findings confirm that Slide2 effectively models leakage losses, making it a reliable tool for leakage estimation in unlined trapezoidal channels. The minimal deviation between the analytical and numerical results supports the validity of the simulation process, ensuring confidence in using the Slide2 model for further leakage analysis under varying channel conditions.

Table 1. Comparison of calculated values of q^* from Equation (6) and the Slide2 model.

b^*	1	2	3	4	5
$q^*_{Eq.\ (6)}$	5.50	6.80	8.00	9.15	10.30
q^*_{Slide2}	5.68	7.04	8.37	9.63	10.92

3.2. Simulation Results

To assess how lining affects the leakage losses ratio (q^*), two main parameters were examined: the liner hydraulic conductivity ratio (k^*) and the ratio of liner thickness to water depth (t^*), which were set at 0.1 and 0.2, respectively. The choice of $k^* = 0.1$ was made as it represents a moderate value within the studied range, ensuring it is neither excessively high nor too low. When k^* values approach 1, the impact of the liner in reducing leakage diminishes, whereas for very low k^* values (≤ 0.01), leakage losses become nearly negligible. Similarly, the decision to use $t^* = 0.2$ was based on the understanding that thicker liners are more effective at preventing leakage compared to thinner ones ($t^* < 0.2$), as they offer a more substantial barrier against water infiltration.

Figure 3 presents the relationship between q^* and different k^* and b^* values while maintaining t^* at 0.2 and z at 1. When t^* was held constant at 0.2, the average reduction in leakage

losses was observed as follows: 8.9%, 20.4%, 67.9%, 82.6%, 96.2%, 97.4%, 99.4%, and 99.7% for k^* values of 0.50, 0.30, 0.10, 0.05, 0.01, 0.005, 0.001, and 0.0005, respectively. Additionally, Figure 4 demonstrates a significant decline in leakage losses as t^* increases. When k^* was fixed at 0.1 with z = 1, the average percentage reduction in leakage losses was recorded as 10%, 23%, 41%, 61%, and 68% for t^* values of 0.02, 0.05, 0.10, 0.15, and 0.20, respectively.

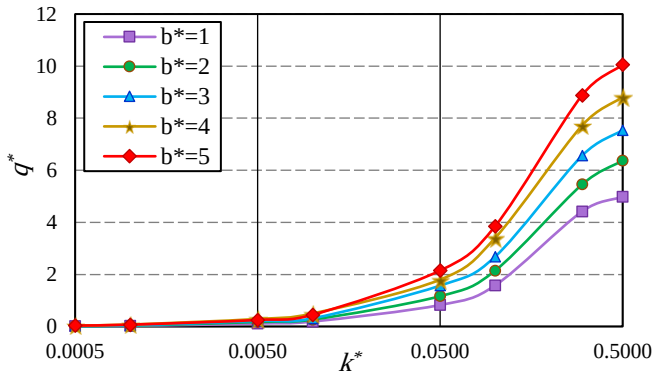

Figure 3. Estimated q^* ratios versus the k^* and b^* ratios (t^* = 0.20 and z = 1).

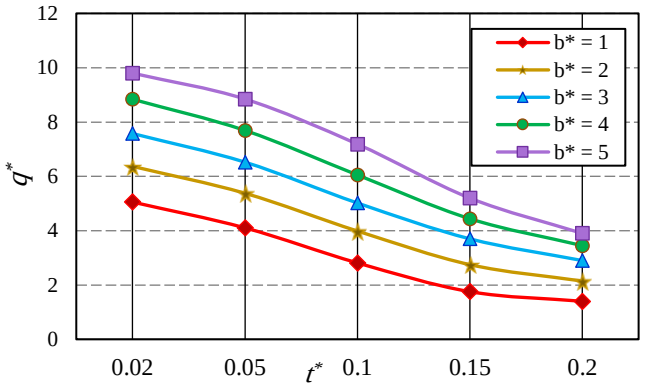

Figure 4. Estimated q^* ratios versus the t^* and b^* ratios (k^* = 0.1 and z = 1).

The impact of side slope values on leakage reduction is depicted in Figure 5, which illustrates the average leakage reduction for various k^* values across different z values. The results show that changes in z have a relatively minor effect on the leakage losses ratio (q^*), as confirmed by the trends observed in Figure 5. With t^* set at 0.2, raising the z value by 0.5 resulted in mean leakage loss reductions of 12.1%, 23.3%, 67.8%, 84.5%, 96.1%, 97.3%, 99.3%, and 99.7% for k^* values of 0.5, 0.3, 0.1, 0.05, 0.01, 0.005, 0.001, and 0.0005, respectively. Similarly, Figure 6 highlights the variation in average leakage reduction across different side slopes for each t^* value. When k^* was fixed at 0.10, increasing z by 0.5 led to a decrease in leakage losses of 9.93%, 22.6%, 41.4%, 61.1%, and 67.8% for t^* values of 0.02, 0.05, 0.10, 0.15, and 0.20, respectively. The results reveal a direct correlation between liner hydraulic conductivity and leakage losses, indicating that liners with higher hydraulic conductivity allow greater water seepage, leading to increased leakage. Conversely, liners with lower hydraulic conductivity effectively limit water loss. Furthermore, the study found an inverse relationship between liner thickness and leakage losses for all tested b^* values, showing that increasing t^* by 0.05 consistently resulted in roughly a 15% reduction in leakage losses, regardless of the z value. Another key finding was the influence of side slopes, where flatter slopes contributed to higher leakage losses compared to steeper ones. This can be attributed to the fact that flatter slopes have a larger wetted perimeter, increasing the surface area available for water leakage. In summary, the findings consistently demonstrate that regardless of the b^* ratio, leakage losses decline as k^* decreases and t^* increases, across all observed side slope values.

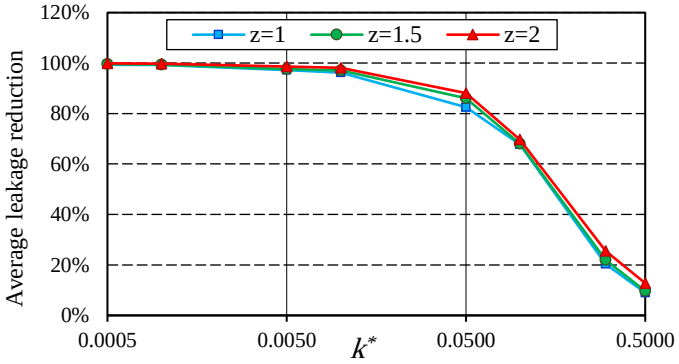

Figure 5. Average % reduction in q^* ratios versus k^* and z ratios (t^* = 0.2).

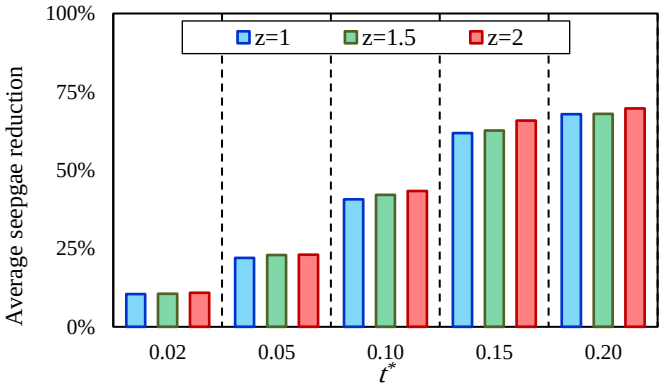

Figure 6. Average % reduction in q^* ratios versus t^* and z ratios (k^* = 0.1).

3.3. Developed MNR equations

3.1.1. Statistical Evaluation

The evaluation of multicollinearity, as presented in Table 2, suggests that while most input variables show high statistical significance, the assumption of the absence of multicollinearity is not entirely supported by the data. The VIF for the intercept is 6.646, which indicates some level of multicollinearity within the model. This suggests redundancy among predictor variables, which may affect the model's stability and interpretation. However, for the variables b^*, z, k^*, and t^*, the VIF values are all 1, implying that these individual variables do not exhibit multicollinearity. Therefore, while the overall model shows some potential issues with multicollinearity, the predictor variables themselves exhibit minimal redundancy.

The results from the ANOVA analysis (Table 2) further confirm that b^*, k^*, and t^* have a significant effect on the model's output. This is evidenced by their high F-statistics and

low p-values, which reflect the high correlation between variations in these geometric and hydraulic parameters and changes in the dependent variable. These parameters are critical in explaining the variability of the model's outcome. On the other hand, the variable z does not demonstrate statistical significance, as its p-value (0.0765) exceeds the conventional 0.05 threshold, indicating that its effect on the model is comparatively weak. Further validation of the input variables' importance is provided by the Z-test results in Table 2. The z-scores for b^*, k^*, and t^* are notably large, which indicates that the observed means for these variables differ significantly from the hypothesized mean of zero. These results are corroborated by the corresponding p-values, which indicate that the z-scores surpass the critical thresholds for both one-tailed (1.64) and two-tailed (1.96) tests, reinforcing the statistical significance of these variables. While the ANOVA test did not identify z as a significant contributor, its Z-test result suggests that its mean remains stable across the sample dataset, hinting at potential relevance in specific modeling contexts.

Table 2. Multicollinearity and hypothesis analyses.

Multicollinearity					
Input Variables	**Intercept**	b^*	z	k^*	t^*
Coefficients	0.879	2.312	0.670	8.894	-2.168
Standard Error	0.200	0.219	0.190	0.225	0.214
T-stat	4.400	10.547	3.529	39.451	-10.149
p-value	0.000	0.000	0.000	0.000	0.000
Lower 95%	0.488	1.882	0.298	8.452	-2.587
Upper 95%	1.271	2.741	1.042	9.336	-1.749
R^2	0.750	0.750	0.750	0.750	0.750
VIF	6.646	1.000	1.000	1.000	1.000

ANOVA test												
	ANOVA for b^*			**ANOVA for z**			**ANOVA for k^***			**ANOVA for t^***		
Variation source	Between groups	Within groups	Total	Between groups	Within groups	Total	Between groups	Within groups	Total	Between groups	Within groups	Total
SS	401	8170	8570	44.9	8520	8570	5610	2960	8570	371	8200	8570
df	1	598	599	1	598	599	1	598	599	1	598	599
MS	401	13.7	-	44.9	14.3	-	5610	4.95	-	371	13.7	-
F-statistic	29.344	-	-	3.148	-	-	1132.68	-	-	27.073	-	-
p-value	8.79E-08	-	-	0.0765	-	-	1.11E-16	-	-	2.70E-07	-	-
F crit	3.8571	-	-	3.8571	-	-	3.8571	-	-	3.8571	-	-

Z-test				
Statistical Parameter	**Mean**	**Known Variance**	**Observations**	**z-Score**
b^*	3.000	2.003	600	51.92
z	1.500	0.167	600	89.92
k^*	0.121	0.030	600	17.22
t^*	0.104	0.004	600	38.98

3.1.2. Individual equations for different channel side slopes

The MNR models developed in this study were assessed at different side slope values (z) to determine their predictive accuracy in estimating leakage losses. The statistical validation of these models was performed using ANOVA, providing insights into their explanatory power and overall reliability. For z=1, Eq. (7) was obtained from the MNR model. The ANOVA results indicated a total sum of squares (SS_{Total}) of 4370.522, with the regression model accounting for 4122.008 and a residual sum of squares of 248.515. This resulted in an R-squared value of 0.895, meaning that 89.5% of the variation in q^* was explained by the model. RMSE was found to be 1.114, confirming the model's ability to capture the relationship between variables with minimal error. The scatter plot in Figure 7a illustrates the relationship between the actual and predicted values of q^*, where most data points are closely aligned with the equality line and within the ±25% deviation boundaries. This alignment confirms that the model provides an accurate estimation of leakage losses for this specific case.

For z=1.5, Eq. (8) was obtained from the MNR model. The ANOVA results revealed that SS_{Total} was 5268.071, with the regression model accounting for 4994.677 and a residual sum of squares of 273.394. The R-squared value increased to 0.903, indicating that 90.3% of the variability in q^* was captured by the model. The RMSE value of 1.169 was slightly higher than that obtained for z=1, but the overall accuracy of the model remained high. Figure 7b presents the scatter plot for this model, showing that data points remained well-distributed

around the equality line. The majority of values were confined within the ±25% deviation range, confirming that the model successfully captures the variability in leakage losses for this particular slope condition.

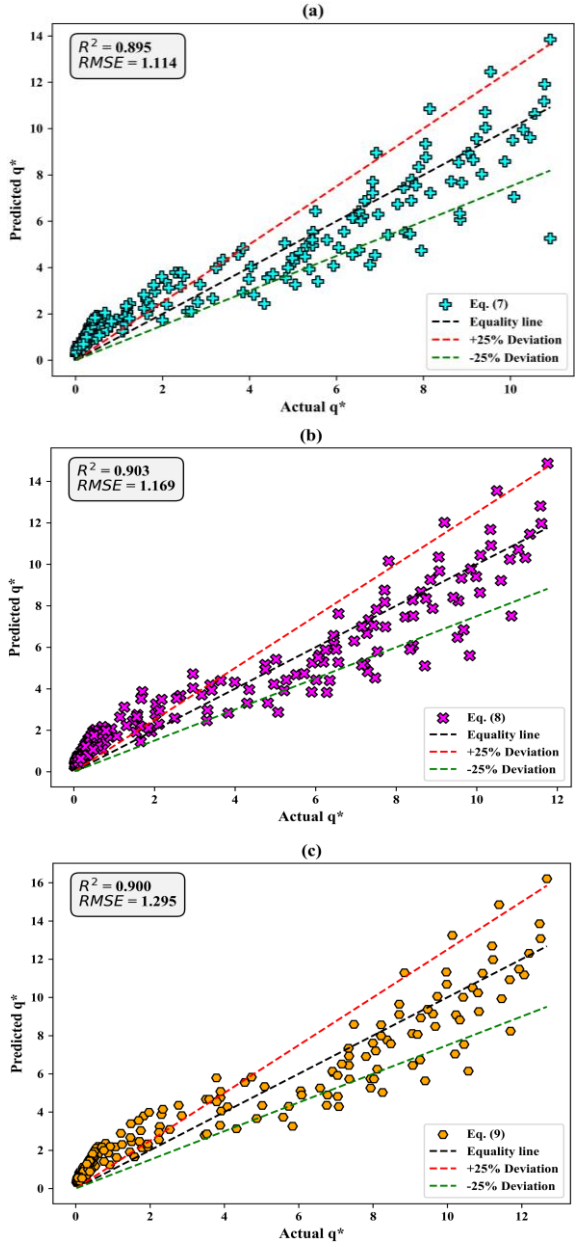

Figure 7. Scatter plots of actual vs. predicted q^* for different side slopes (z): **(a)** z=1, **(b)** z=1.5, and **(c)** z=2. The black dashed line represents equality, while red and green indicate ±25% deviation.

For z=2, Eq. (9) was obtained from the MNR model. The ANOVA results indicated that SS_{Total} was 6282.117, with the regression model explaining 5946.530 and the residual sum of squares amounting to 335.587. The R-squared value remained high at 0.900, confirming that 90.0% of the variation in q^* was accounted for by the model. The RMSE was found to be 1.295, slightly increasing the residual error compared to the previous cases. Despite this, the scatter plot in Figure 7c confirmed that the model remained highly reliable, with most predicted values closely following the equality line and falling within the ±25% deviation range. This result suggests that as the slope value increases, the model remains robust, with only slight variations in prediction accuracy.

The overall analysis confirms that all three models show high statistical significance, as reflected in their high R-squared values and relatively low residual errors. The scatter plots further reinforce the validity of these models by illustrating that the predicted values align closely with the actual values, demonstrating minimal deviations. The consistent performance across different side slope values suggests that the MNR approach effectively captures leakage loss behavior under varying conditions. The equations governing these models are compiled as follows:

$$q^* = b^{*0.476} \times k^{*0.420} \times t^{*-0.164} \times 4.535 \quad for\ z = 1 \qquad (7)$$

$$q^* = b^{*0.415} \times k^{*0.424} \times t^{*-0.162} \times 5.422 \quad for\ z = 1.5 \qquad (8)$$

$$q^* = b^{*0.395} \times k^{*0.421} \times t^{*-0.171} \times 5.880 \quad for\ z = 2 \qquad (9)$$

3.1.3. Generalized MNR equation for all channel side slopes

The generalized MNR equation (Eq. 10) for all side slope values (z) is expressed as:

$$q^* = b^{*0.423} \times z^{0.265} \times k^{*0.422} \times t^{*-0.166} \times 4.791 \qquad (10)$$

where b^*, z, k^*, and t^* represent the independent variables influencing the predicted leakage loss, and the estimated coefficients define the extent of their impact. The statistical analysis of this generalized model was performed using ANOVA, which confirmed its high predictive capability. The SS_{Total} was calculated as 15,920.71, with the regression model explaining 15,059.18 of this variance, leaving only 861.53 as the residual sum of squares. This resulted in an R-squared value of 0.899, indicating that 89.9% of the variability in q^* is accounted for by the model. The RMSE was found to be 1.448, reflecting the model's accuracy in capturing the relationships between variables with a minimal level of error.

The parameter estimates provide insights into the influence of each independent variable on the predicted outcome. The coefficient 0.423 associated with b^* suggests that an increase in this variable leads to a significant positive effect on q^*. Similarly, the coefficient 0.265 for z indicates a positive correlation, though its impact is less pronounced than that of b^*. The coefficient 0.422 for k^* further reinforces its high contribution to predicting leakage losses. However, the coefficient -0.166 for t^* signifies a negative relationship, implying that higher values of t^* lead to a slight reduction in q^*. The constant 4.791 ensures that the model is well-calibrated and maintains appropriate scaling across different scenarios.

The scatter plot in Figure 8 illustrates the comparison between actual and predicted values of q^* using the generalized regression model. The alignment of data points along the equality line suggests a high correlation between the predicted and actual leakage loss values. The presence of most data points within the ±25% deviation range confirms that the model maintains high predictive accuracy across varying side slope values. The R-squared value of 0.899, as shown in the figure, highlights the model's robustness and reliability, ensuring that it can be effectively applied to different slope

conditions without significant loss of precision. The inclusion of deviation boundaries in the plot further reinforces the accuracy of the model, as the majority of predicted values remain within acceptable margins of deviation.

Overall, the analysis confirms that the generalized MNR model effectively captures the relationship between leakage losses and the governing parameters across different values of *z*. The high R-squared value, combined with the minimal residual error, supports the validity of the model. The scatter plot further verifies that the model consistently aligns with observed data, reinforcing its suitability for predicting leakage losses under various side slope conditions.

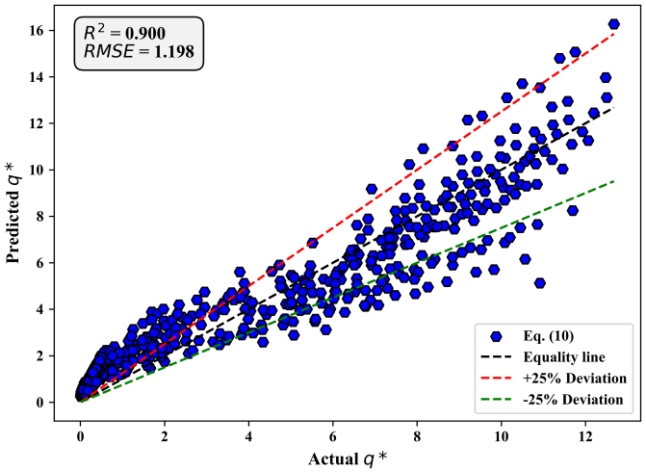

Figure 8. Scatter plot of actual vs. predicted q^* using the generalized MNR model for all side slopes (*z*). The black dashed line represents the equality line, while the red and green dashed lines indicate ±25% deviation.

4. Conclusions

This study analyzed seepage losses in trapezoidal canals using the Slide2 numerical model and developed MNR equations to enhance predictive accuracy. The validation of the Slide2 model against an analytical solution demonstrated its reliability, with deviations ranging from 3% to 6%. The simulation results emphasized the significant influence of liner properties on seepage losses, highlighting that lower hydraulic conductivity ratio (k^*) effectively minimizes leakage, while increasing liner thickness (t^*) further enhances seepage reduction. Additionally, the effect of side slope (*z*) was examined, confirming that steeper slopes lead to reduced seepage losses due to a smaller wetted perimeter. Summing up the conclusions, the following key findings can be drawn:

- The Slide2 model successfully simulated seepage losses, showing high agreement with analytical solutions, validating its effectiveness for seepage analysis.
- Lowering the liner hydraulic conductivity and increasing liner thickness significantly reduce seepage losses, demonstrating the importance of optimized liner design in canal systems.
- The influence of side slopes was evident, with steeper slopes leading to lower seepage losses by reducing the wetted perimeter and, consequently, the seepage pathway.
- Individual MNR equations were developed for different side slopes (*z*), achieving high predictive accuracy with R^2 values exceeding 0.89. The generalized equation, applicable to all side slopes, exhibited an R^2 of 0.899 and an RMSE of 1.448, demonstrating robust model performance.
- The scatter plots confirmed the high correlation between predicted and actual seepage losses, with the majority of data points falling within ±25% deviation, validating the reliability of the developed MNR models.

Statements and Declarations

Acknowledgements

The author sincerely thanks and expresses deep gratitude to the Civil Engineering Department, Faculty of Engineering, Horus University–Egypt, for their invaluable support and for facilitating the laboratory work throughout the research period.

Authors Contributions

The author confirms sole responsibility for the following: study conception and design, data collection, analysis and interpretation of results, and manuscript preparation.

Funding

This research received no external funding.

Conflicts of Interest

The author reported no potential conflict of interest.

Data availability statement

Data, models, or codes that support the findings of this study are available from the corresponding author upon reasonable request.

References

[1] A. A. R. Lund, T. K. Gates, and J. Scalia, "Characterization and control of irrigation canal seepage losses: A review and perspective focused on field data," *Agric. Water Manag.*, vol. 289, p. 108516, Nov. **2023**, doi: 10.1016/j.agwat.2023.108516.

[2] G. Zakir-Hassan *et al.*, "Evaluation of hydraulic efficiency of lined irrigation channels–a case study from Punjab, Pakistan," *Hydrol. Res.*, vol. 54, no. 4, pp. 523–546, **2023**, doi: 10.2166/NH.2023.105.

[3] M. R. Kumar and D. Subhasish, "Hydraulics of Seepage from Trapezoidal Channels," *J. Hydraul. Eng.*, vol. 146, no. 12, p. 4020083, Dec. **2020**, doi: 10.1061/(ASCE)HY.1943-7900.0001825.

[4] M. K. Elshaarawy, "Metaheuristic-driven CatBoost model for accurate seepage loss prediction in lined canals," *Multiscale Multidiscip. Model. Exp. Des.*, vol. 8, no. 5, p. 235, May **2025**, doi: 10.1007/s41939-025-00800-8.

[5] M. G. Eltarabily, M. K. Elshaarawy, M. Elkiki, and T. Selim, "Modeling Surface Water and Groundwater Interactions for Seepage Losses Estimation from Unlined and Lined Canals," *Water Sci.*, vol. 37, no. 1, pp. 315–328, **2023**, doi: 10.1080/23570008.2023.2248734.

[6] M. Aslam *et al.*, "Seepage and Groundwater Numerical Modelling for Managing Waterlogging in the Vicinity of the Trimmu–Sidhnai Link Canal," *Infrastructures*, vol. 7, no. 10, p. 144, Oct. **2022**, doi: 10.3390/infrastructures7100144.

[7] M. Mutema and K. Dhavu, "Review of factors affecting canal water losses based on a meta-analysis of worldwide data," *Irrig. Drain.*, vol. 71, no. 3, pp. 559–573, **2022**, doi: 10.1002/ird.2689.

[8] M. Zeleňáková, A. Arifjanov, H. F. Abd-Elhamid, M. B. Gergeľová, A. Fatxulloyev, and D. Allayorov, "The Effect of Lining Hydraulic Properties on the Efficiency and Cost of Irrigation Canal Reconstruction," *Water Resour. Manag.*, Apr. **2025**, doi: 10.1007/s11269-025-04218-2.

[9] E. Elkamhawy, M. Zelenakova, and I. Abd-Elaty, "Numerical canal seepage loss evaluation for different lining and crack techniques in arid and semi-arid regions: A case study of the river nile, Egypt," *Water (Switzerland)*, vol. 13, no. 21, **2021**, doi: 10.3390/w13213135.

[10] I. Abd-Elaty, L. Pugliese, K. M. Bali, M. E. Grismer, and M. G. Eltarabily, "Modelling the impact of lining and covering irrigation canals on underlying groundwater stores in the Nile Delta, Egypt," *Hydrol. Process.*, vol. 36, no. 1, p. e14466, Jan. **2022**, doi: 10.1002/hyp.14466.

[11] F. B. Sarand and M. Hajialilue-Bonab, "Effect of Unsaturated Expansive Soils on Canal Linings: A Case Study on the Tabriz Plain Canal, Iran," *Irrig. Drain.*, vol. 66, no. 3, pp. 396–410, Jul. **2017**, doi: 10.1002/ird.2113.

[12] H. Plusquellec, "Overestimation of benefits of canal irrigation projects: decline of performance over time caused by deterioration of concrete canal lining," *Irrig. Drain.*, vol. 68, no. 3, pp. 383–388, Jul. **2019**, doi: 10.1002/ird.2341.

[13] M. A. Ashour, M. S. Abdel Nasser, and T. S. Abu-Zaid, "Field Study to Evaluate Water Loss in the Irrigation Canals of Middle Egypt: A Case Study of the Al Maanna Canal and Its Branches, Assiut Governorate," *Limnol. Rev.*, vol. 23, no. 2, pp. 70–92, Aug. **2023**, doi: 10.3390/limnolrev23020005.

[14] D. A. El-Molla and M. G. Eltarabily, "Estimation of seepage losses from cracked rigid canal liners using finite element modeling," *J. Appl. Water Eng. Res.*, **2023**, doi: 10.1080/23249676.2023.2233904.

[15] Z. Shah, H. Gabriel, S. Haider, and T. Jafri, "Analysis of seepage loss from concrete lined irrigation canals in Punjab, Pakistan," *Irrig. Drain.*, vol. 69, no. 4, pp. 668–681, **2020**, doi: 10.1002/ird.2474.

[16] R. Hosseinzadeh Asl, F. Salmasi, and H. Arvanaghi, "Numerical investigation on geometric configurations affecting seepage from unlined earthen channels and the comparison with field measurements," *Eng. Appl. Comput. Fluid Mech.*, vol. 14, no. 1, pp. 236–253, **2020**, doi: 10.1080/19942060.2019.1706639.

[17] F. Salmasi and J. Abraham, "Predicting seepage from unlined earthen channels using the finite element method and multi variable nonlinear regression," *Agric. Water Manag.*, vol. 234, no. November **2019**, p. 106148, 2020, doi: 10.1016/j.agwat.2020.106148.

[18] F. Solomon and S. Ekolu, "Effect of clay-concrete lining on canal seepage towards the drainage region - an analysis using Finite-Element method," *Constr. Mater. Struct.*, pp. 1331–1341, **2014**, doi: https://ebooks.iospress.nl/doi/10.3233/978-1-61499-466-4-1331.

[19] A. A. J. Jamel, "Analysis and Estimation of Downward Seepage from Lining and Unlining Triangular Open Channel," *Eng. Technol. J.*, vol. 34, no. 2, pp. 406–419, Feb. **2016**, doi: 10.30684/etj.34.2A.18.

[20] E. Tavakoli, B. Ghorbani, and B. Gh, "Seepage Estimation in Water Conveyance Canals by Emirical Equations and SEEP/W model," *J. Water Res. Agric.*, vol. 31, no. 3, pp. 425–440, **2017**, doi: 10.22092/jwra.2017.113677.

[21] M. M. Rezapour Tabari, S. Tavakoli, and M. Mazak Mari, "Optimal Design of Concrete Canal Section for Minimizing Costs of Water Loss, Lining and Earthworks," *Water Resour. Manag.*, vol. 28, no. 10, pp. 3019–3034, Aug. **2014**, doi: 10.1007/s11269-014-0652-9.

[22] M. Mohammad Rezapour Tabari and M. Mazak Mari, "The Integrated Approach of Simulation and Optimization in Determining the Optimum Dimensions of Canal for Seepage Control," *Water Resour. Manag.*, vol. 30, no. 3, pp. 1271–1292, Feb. **2016**, doi: 10.1007/s11269-016-1225-x.

[23] S. M. . Sharief and M. Zakwan, "Comparative analysis of seepage loss through different canal linings," *Int. J. Hydrol. Sci. Technol.*, vol. 1, no. 1, p. 1, **2021**, doi: 10.1504/ijhst.2021.10037172.

[24] D. A. El-Molla and M. A. El-Molla, "Reducing the conveyance losses in trapezoidal canals using compacted earth lining," *Ain Shams Eng. J.*, vol. 12, Feb. **2021**, doi: 10.1016/j.asej.2021.01.018.

[25] M. G. Eltarabily, M. K. Elshaarawy, M. Elkiki, and T. Selim, "Computational fluid dynamics and artificial neural networks for modelling lined irrigation canals with low-density polyethylene and cement concrete liners," *Irrig. Drain.*, vol. 73, no. 3, pp. 910–927, Jul. **2024**, doi: 10.1002/ird.2911.

[26] M. Elshaarawy, A. K. Hamed, and S. Hamed, "Regression-Based Models for Predicting Discharge Coefficient of Triangular Side Orifice," *J. Eng. Res.*, vol. 7, no. 5, pp. 224–231, Nov. **2023**, doi: digitalcommons.aaru.edu.jo/erjeng/vol7/iss5/31.

[27] M. M. Alsaadawi, M. K. Elshaarawy, and A. K. Hamed, "Concrete compressive strength classification using hybrid machine learning models and interactive GUI," *Innov. Infrastruct. Solut.*, vol. 10, no. 5, p. 198, May **2025**, doi: 10.1007/s41062-025-01983-2.

[28] P. Khosravinia, M. R. Nikpour, O. Kisi, and R. M. Adnan, "Predicting Discharge Coefficient of Triangular Side Orifice Using LSSVM Optimized by Gravity Search Algorithm," *Water*, vol. 15, no. 7, p. 1341, Mar. **2023**, doi: 10.3390/w15071341.

[29] G. Shen, S. Li, A. Parsaie, G. Li, D. Cao, and P. Pandey, "Prediction and parameter quantitative analysis of side orifice discharge coefficient based on machine learning," *Water Supply*, vol. 22, no. 12, pp. 8880–8892, Nov. **2022**, doi: 10.2166/ws.2022.394.

[30] M. Gad, H. M. Abdelhaleem, and W. O. A. S., "Forecasting the seepage loss for lined and un-lined canals using artificial neural network and gene expression programming," *Geomatics, Nat. Hazards Risk*, vol. 14, no. 1, p. 2221775, Dec. **2023**, doi: 10.1080/19475705.2023.2221775.

[31] T. Selim, M. K. Elshaarawy, M. Elkiki, and M. G. Eltarabily, "Estimating seepage losses from lined irrigation canals using nonlinear regression and artificial neural network models," *Appl. Water Sci.*, vol. 14, no. 5, p. 90, May **2024**, doi: 10.1007/s13201-024-02142-1.

[32] Rocscience, "Slide 5.0 User's Guide," *Slide 5.0 User's Guide*, p. 90, **2002**. Avaiable online at: https://www.rocscience.com/downloads/slide/Slide_TutorialManual.pdf.

[33] Rocscience, "Groundwater Module in Slide 2D finite element program for groundwater analysis," **2002**. https://www.rocscience.com/help/slide2/documentation/program-overview/groundwater-analysis-with-slide2.

[34] M. K. Elshaarawy, M. Elkiki, T. Selim, and M. G. Eltarabily, "Hydraulic Comparison of Different Types of Lining for Irrigation Canals Using Computational Fluid Dynamic Models," M.Sc. Thesis, Civil Engineering Department, Faculty of Engineering, Port Said University., **2024**. [Online]. Available: http://dx.doi.org/10.13140/RG.2.2.21927.97441

[35] J. H. Evans, "Dimensional Analysis and the Buckingham Pi Theorem," *Am. J. Phys.*, vol. 40, no. 12, pp. 1815–1822, Dec. **1972**, doi: 10.1119/1.1987069.

[36] M. G. Eltarabily, H. F. Abd-Elhamid, M. Zeleňáková, M. K. Elshaarawy, M. Elkiki, and T. Selim, "Predicting seepage losses from lined irrigation canals using machine learning models," *Front. Water*, vol. 5, **2023,** doi: 10.3389/frwa.2023.1287357.

[37] M. K. Elshaarawy and N. H. Elmasry, "Experimental and Numerical Modeling of Seepage in Trapezoidal Channels," *Knowledge-Based Eng. Sci.*, vol. 5, no. 3, pp. 43–60, Dec. **2024**, doi: 10.51526/kbes.2024.5.3.43-60.

[38] M. K. Elshaarawy, N. H. Elmasry, T. Selim, M. Elkiki, and M. G. Eltarabily, "Determining Seepage Loss Predictions in Lined Canals Through Optimizing Advanced Gradient Boosting Techniques," *Water Conserv. Sci. Eng.*, **2024**, doi: 10.1007/s41101-024-00306-3.

[39] V. V Vedernikov, "Theory of seepage and its application in irrigation and drainage," *Gosstrojizdat, Moscow*, **1939**.

[40] Rocscience, "Slide2: Slide Groundwater Verification Manual," **2002**. Available online at: https://www.rocscience.com/help/slide2/verification-theory/verification-manuals.

[41] M. E. Harr, *Groundwater and seepage*. Courier Corporation, **1991**. Avaiable online at: https://istasazeh-co.com/wp-content/uploads/2022/10/Groundwater-and-Seepage-Harr-1990.pdf.

[42] M. K. Elshaarawy and A. K. Hamed, "Machine learning and interactive GUI for estimating roller length of hydraulic jumps," *Neural Comput. Appl.*, Dec. **2024,** doi: 10.1007/s00521-024-10846-3.

[43] Q. L. Lang, G. J. Li, and J. L. Huang, "Application of multiple nonlinear regression based on SPSS in the risk assessment of debris flow," *Adv. Mater. Res.*, vol. 753–755, pp. 3205–3208, **2013**, doi: 10.4028/www.scientific.net/AMR.753-755.3205.

[44] M. K. Elshaarawy and A. K. Hamed, "Modeling hydraulic jump roller length on rough beds: a comparative study of ANN and GEP models," *J. Umm Al-Qura Univ. Eng. Archit.*, **2025**, doi: 10.1007/s43995-024-00093-x.

[45] M. K. Elshaarawy, "Stacked-based hybrid gradient boosting models for estimating seepage from lined canals," *J. Water Process Eng.*, vol. 70, p. 106913, Feb. **2025**, doi: 10.1016/j.jwpe.2024.106913.

[46] F. Yu *et al.*, "Predicting axial load capacity in elliptical fiber reinforced polymer concrete steel double skin columns using machine learning," *Sci. Rep.*, vol. 15, no. 1, p. 12899, Apr. **2025**, doi: 10.1038/s41598-025-97258-y.

[47] M. K. Elshaarawy and A. M. Armanuos, "Predicting Seawater Intrusion Wedge Length in Coastal Aquifers Using Hybrid Gradient Boosting Techniques," *Earth Sci. Informatics*, **2025**, doi: 10.1007/s12145-025-01755-7.

[48] F. Shen, I. Jha, H. F. Isleem, W. J. K. Almoghayer, M. Khishe, and M. K. Elshaarawy, "Advanced predictive machine and deep learning models for round-ended CFST column," *Sci. Rep.*, vol. 15, no. 1, p. 6194, **2025**, doi: 10.1038/s41598-025-90648-2.

[49] A. K. Hamed, M. K. Elshaarawy, and M. M. Alsaadawi, "Stacked-based machine learning to predict the uniaxial compressive strength of concrete materials," *Comput. Struct.*, vol. 308, p. 107644, Feb. **2025**, doi: 10.1016/j.compstruc.2025.107644.

[50] J. Zhang, W. J. K. Almoghayer, H. F. Isleem, B. S. Negi, H. A. Mahmoud, and M. K. Elshaarawy, "Machine learning for the prediction of the axial load-carrying capacity of FRP reinforced hollow concrete column," *Struct. Concr.*, Mar. **2025**, doi: https://doi.org/10.1002/suco.202400886.